Original Article

Pancreatic β-Cells Secrete Insulin in Fast- and Slow-Release Forms

Darren J. Michael,[1] Robert A. Ritzel,[2] Leena Haataja,[3] and Robert H. Chow[1]

Insulin vesicles contain a chemically rich mixture of cargo that includes ions, small molecules, and proteins. At present, it is unclear if all components of this cargo escape from the vesicle at the same rate or to the same extent during exocytosis. Here, we demonstrate through real-time imaging that individual rat and human pancreatic β-cells secrete insulin in heterogeneous forms that disperse either rapidly or slowly. In healthy pancreatic β-cells maintained in culture, most vesicles discharge insulin in its fast-release form, a form that leaves individual vesicles in a few hundred milliseconds. The fast-release form of insulin leaves vesicles as rapidly as C-peptide leaves vesicles. Healthy β-cells also secrete a slow-release form of insulin that leaves vesicles more slowly than C-peptide, over times ranging from seconds to minutes. Individual β-cells make vesicles with both forms of insulin, though not all vesicles contain both forms of insulin. In addition, we confirm that insulin vesicles store their cargo in two functionally distinct compartments: an acidic solution, or halo, and a condensed core. Thus, our results suggest two important features of the condensed core: *1*) It exists in different states among the vesicles undergoing exocytosis and *2*) its dissolution determines the availability of insulin during exocytosis. *Diabetes* 55:600–607, 2006

Insufficient insulin secretion in the face of insulin resistance leads to the disease type 2 diabetes (1). The mechanism responsible for insufficient insulin secretion remains unclear. Before it is possible to understand why insulin secretion fails to compensate for insulin resistance during the progression of type 2 diabetes (2), it is essential to understand insulin secretion at all levels of biological complexity, ranging from the whole pancreas within a living animal to the pancreatic β-cell and its fundamental unit of secretion, the insulin secretory vesicle.

Insulin vesicles contain a chemically complex mixture of ions, small molecules, and proteins (3,4). Among the ions, there are large amounts of two divalent cations: zinc and calcium (5). Both of these ions are believed to play important roles in the regulated secretion of insulin (6). Among the vesicle proteins, insulin-related peptides comprise ~75% of the mass (7). The remaining 25% of the protein mass includes more than a hundred different membrane and cargo proteins. Although our understanding of regulated secretion of insulin has progressed greatly in recent years, the mechanisms that control the trafficking, processing, and secretion of insulin vesicle cargo are still matters of debate and extensive research (8).

Previously, we (9) and others (10–13) have studied secretion from single insulin vesicles by imaging fluorescently tagged proteins consisting of a vesicle cargo protein linked to a fluorescent protein. The fluorescently tagged vesicle cargo proteins, hereafter referred to as fluorescent cargo proteins, have provided a valuable and powerful tool for studies of single vesicle exocytosis. However, as with any new probe for studying exocytosis, it is essential to understand the behavior of the probe before drawing conclusions about the behavior of native vesicle cargo. We have previously compared the behavior of several fluorescent cargo proteins and demonstrated that different fluorescent cargo proteins behave differently during exocytosis. Some fluorescent cargo proteins leave vesicles rapidly and completely, while others persist at the site of exocytosis. In fact, we have found that the design of a fluorescent cargo protein determines its behavior during exocytosis (9). This result suggests that fluorescent cargo proteins do not report the fate of native cargo during exocytosis and leaves open the question of what happens to the native cargo of an insulin vesicle during exocytosis. We address this question here, taking advantage of fluorescent dyes that, as we demonstrate, can stain insulin vesicle dense cores and track dispersion of native insulin vesicle cargo.

According to the simplest model of insulin vesicle exocytosis, a vesicle fuses with the plasma membrane and then releases all of its cargo rapidly and completely (14,15). If all insulin vesicles behaved according to the simplest model of exocytosis, then insulin vesicles should release approximately equal quantities of insulin and C-peptide, an insulin-processing fragment also stored in insulin vesicles. An early study (16) demonstrated nearly equimolar release of newly synthesized rat insulin and C-peptide.

The simplest model of insulin vesicle exocytosis, however, fails to explain a curious feature of pancreatic β-cells: when human and rat pancreatic islet cells are maintained in primary culture, insulin is found on the surface of some β-cells (17–19) but not on the surface of other types of islet cells. Several observations suggest that

From the [1]Department of Physiology and Biophysics, Keck School of Medicine, Zilkha Neurogenetic Institute, University of Southern California, Los Angeles, California; the [2]Department of Endocrinology, University of Heidelberg, Heidelberg, Germany; and the [3]Department of Endocrinology, Larry Hillblom Islet Research Center, University of California, Los Angeles, California.

Address correspondence and reprint requests to Robert H. Chow, University of Southern California, Department of Physiology and Biophysics, 1501 San Pablo St., ZNI 323, Los Angeles, CA 90089. E-mail: rchow@usc.edu.

Received for publication 16 August 2005 and accepted in revised form 15 December 2005.

Additional information for this article can be found in an online appendix available at http://diabetes.diabetesjournals.org.

GFP, green fluorescent protein; TIRF, total internal reflection fluorescence.

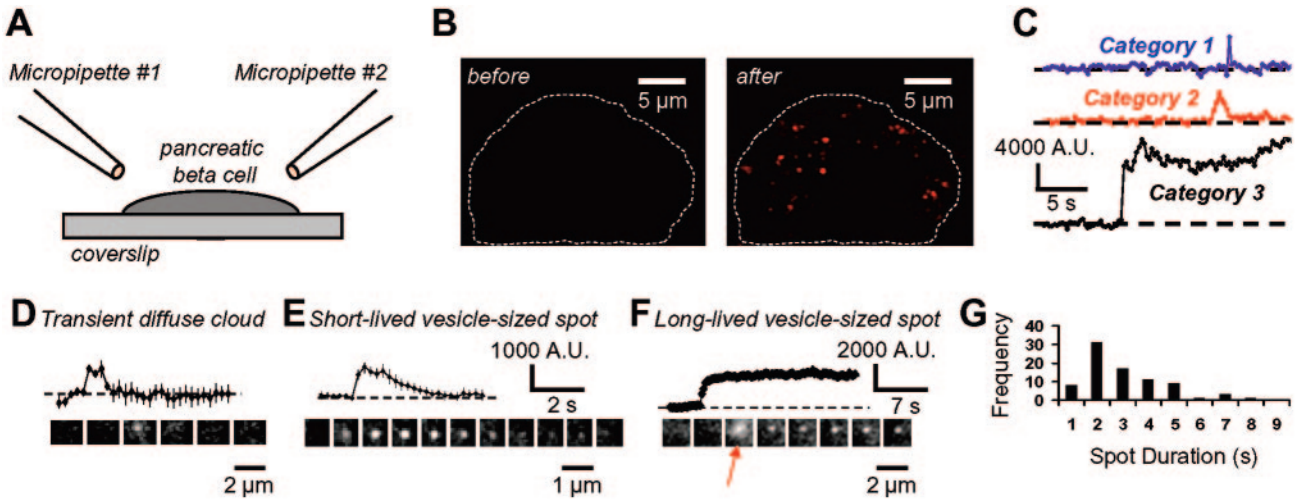

FIG. 1. Native cargo leaves insulin vesicles at widely varying rates. *A*: Experimental setup (see RESEARCH DESIGN AND METHODS). *B*: A β-cell shown before and after stimulation in the presence of fluorescent zinc indicator. *C*: Fluorescence intensity traces for three newly appearing spots. *D–F*: Individual spots fit three patterns of fluorescence change (see labels and text). Traces are averages of representative vesicles (*n* = [vesicles, cells]: *D* [5,3], *E* [11,3], and *F* [14,3]). Montages show either consecutive images (*D* and *E*; 0.25 s per frame) or every 10th image (*F*; 2.5 s per frame). The arrow in *F* highlights a cloud of fluorescence that preceded the vesicle-sized spot. *G*: Duration histogram for short-lived vesicle-sized spots (*n* = 83 vesicles, 8 cells).

cell surface insulin originates from exocytosis. First, exogenously added insulin does not aggregate on a β-cell's plasma membrane (17). Second, the fraction of β-cells with insulin on their surface increases as a function of time (17), in particular when cells are exposed to factors known to enhance the regulated secretion of insulin—theophylline and elevated extracellular concentrations of calcium and glucose (17). Third, cell surface insulin is not distributed uniformly around the cell's perimeter; instead, it is found in discrete spots (17–19). Finally, images from ultrastructural techniques such as electron microscopy and autometallography have shown what appear to be insulin-dense cores outside of pancreatic β-cells (18,20). Although this evidence suggests that cell surface insulin arises from dense core material released during exocytosis, these studies did not determine what happens to the dense core material, i.e., how often does an insulin-dense core remain at the site of exocytosis, how long does an insulin-dense core remain at the cell surface after exocytosis, and what is the ultimate fate of the cargo stored in an insulin-dense core?

The fate of an insulin vesicle's cargo can be resolved by directly comparing secretion kinetics for different types of cargo stored within the same insulin vesicle. We make the comparison here, for the first time. To monitor insulin vesicle exocytosis, we used two independent markers that report exocytosis: a fluorescent cargo protein and a fluorescent zinc indicator (21). Examined separately, neither of these probes was able to faithfully track the fates of all native cargo. Examined together, however, they revealed novel features of insulin vesicle exocytosis. Specifically, we found that different vesicles release their native cargo at different rates. Most vesicles in healthy pancreatic β-cells secrete insulin in its fast-release form, a form of insulin that leaves vesicles as rapidly as C-peptide. Other vesicles, however, secrete a slow-release form of insulin that disperses over seconds to minutes. Thus, the population of insulin vesicles inside a single β-cell is heterogeneous.

RESEARCH DESIGN AND METHODS

Tissue collection and cell culture. Human islets were obtained through the Islet Cell Resource Centers (City of Hope, Duarte, CA). Rat pancreatic β-cells were prepared and cultured as described (9). Dispersed cells were used within 5 days. Rat and human β-cells were treated identically except for the concentration of glucose in culture medium (8 vs. 5 mmol/l, respectively).

Vectors and adenovirus. Construction (22,23) and use (9) of adenovirus containing the gene for insulin C-peptide fused to emerald green fluorescent protein (GFP) have been described.

Solutions and chemicals. Extracellular solution used in imaging experiments was composed of the following (in mmol/l): 136 NaCl, 4.2 KCl, 2.4 $CaCl_2$, 1.2 $MgSO_4$, 1.2 KH_2PO_4, 1 L-glutamine, 4 glucose, and 10 HEPES (pH 7.4). In the stimulating solution, an equal quantity of KCl replaced NaCl to yield a final potassium concentration of 50 mmol/l. All solutions were prepared with water from a commercial purification system (Nanopure Infinity; Barnstead Thermolyne, Dubuque, IA). The osmolalities of extracellular and stimulating solutions were matched and fell between 280 and 320 mOsm. All salts for solutions were obtained from Sigma Aldrich (St. Louis, MO) with the highest purity available. Fluorescent zinc indicators were from Invitrogen (Carlsbad, CA) (Newport Green DCF [green]; Fig. 1*C–G* and Fig. 2*F–H*; online appendix Fig. S1 [available from http://diabetes.diabetesjournals.org] and Rhodzin [red]; Fig. 1*B*; Fig. 2*A–E*; Fig. 3*C–I*; Fig. 4; online appendix Fig. S2). Stock solutions for zinc indicators were prepared in deionized water.

Total internal reflection fluorescence imaging. We have previously published the details for our total internal reflection fluorescence (TIRF) microscope (9). For two-color TIRF microscopy (24,25), we added the following components: *1*) helium-neon laser (543 nm; JDS Uniphase, San Jose, CA), *2*) dichroic mirror (530 dclp; Chroma, Rockingham, VT), *3*) dichroic mirror (XF2046; Omega, Brattleboro, VT), and *4*) dual-emission pathway (DualView, equipped with dichroic mirror [560 dcxr, Chroma] and emission filters [HQ515/30, Chroma and D605/55, Chroma]; Optical Insights, Santa Fe, NM). Before and after each two-color TIRF experiment, we imaged a field of stationary beads labeled with multiple fluorescent dyes (200 nm diameter, TetraSpeck, Invitrogen). For most beads, red and green fluorescence profiles agreed within 1 pixel in both the x- and y-axis. If an adjustment was necessary to align red and green fluorescence profiles for beads at a given location, a similar adjustment was applied to the same regions for all images when we analyzed data from the corresponding experiments. Throughout the imaging experiments, cells were maintained in a warmed solution (between 35 and 37°C) with continuous exchange (~1 ml/min). Pulled glass pipettes (~3-μm tip diameter) were positioned near cells for transient application of test solutions. Insulin-zinc crystals and live cells labeled with antibody (see below) were imaged at room temperature (~25°C).

Solutions for fluorescent zinc indicator. Fluorescent zinc indicators were used at a final concentration between 5 and 12 μmol/l. When cells were stimulated in the presence of fluorescent zinc indicator, two micropipettes were positioned next to the cell cluster (Fig. 1*A*). The first pipette was used to apply extracellular solution spiked with fluorescent zinc indicator, and the second was used to apply stimulating solution that also contained fluorescent zinc indicator.

Insulin-zinc crystals. Insulin and zinc were crystallized using a standard protocol (26,27). Single rhombohedral crystals were selected for study and

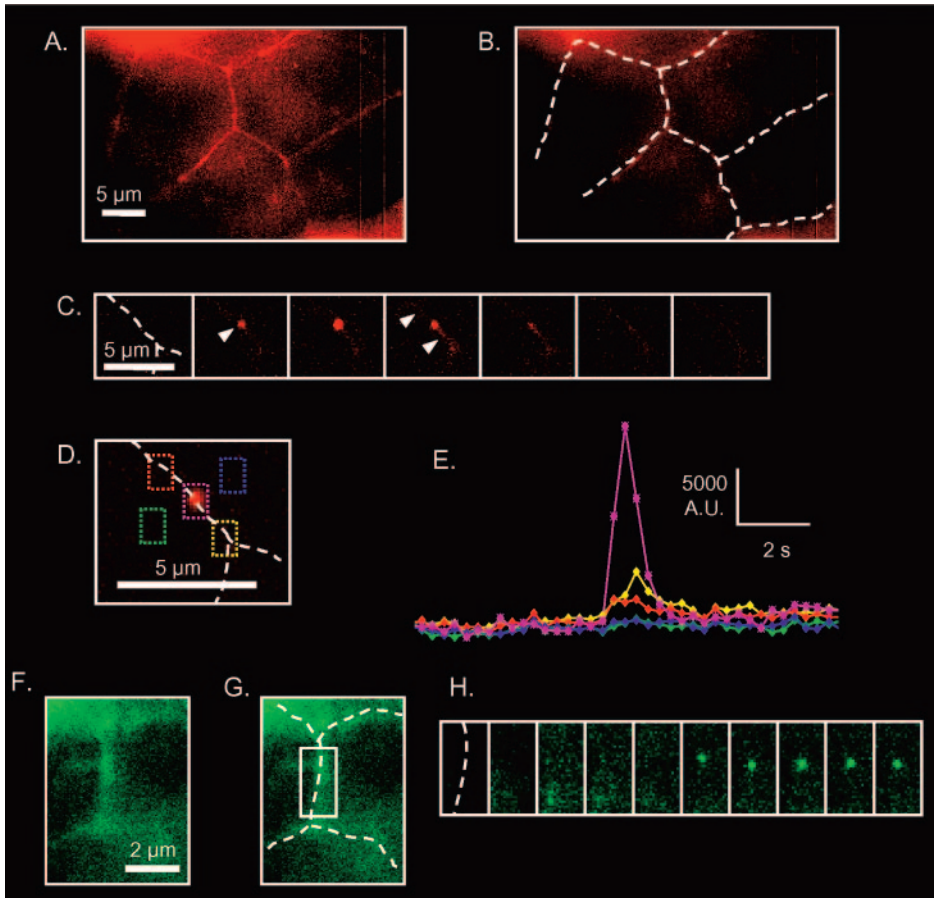

FIG. 2. Native cargo, released between cells, also leaves insulin vesicles at widely varying rates. *A* and *B*: Zinc dye (Rhodzin) in spaces between cells (~3 μm above the coverslip) (*A* and *B*, same scale bar). *C*: Short-lived vesicle-sized spot (sequential frames shown; ~200 ms per frame). *D* and *E*: Fluorescence intensity increased asymmetrically around the original spot shown in *C*. Average fluorescence intensity was plotted for each of the five regions of interest shown. Scale bar, 5 μm. *F* and *G*: Zinc dye (Newport Green) in the spaces between cells. *H*: Long-lived vesicle-sized spot (~7 s between frames) (*F*–*H*, same scale bar). Intensity scales in panels *A*, *B*, *F*, and *G* were adjusted to emphasize the faint but detectable background fluorescence of the zinc indicator.

positioned in the field of view for fluorescence imaging. To investigate kinetics for entry and exit of fluorescent zinc indicator (Rhodzin), two micropipettes were placed next to a single insulin crystal. First, the crystal was perifused with external buffer that contained dye and then washed continuously with a vigorous stream of dye-free external buffer. In these studies, we examined the dye's behavior both at the base of the crystal, using TIRF microscopy, and at planes above the base of the crystal, using both widefield and multiphoton fluorescence microscopy. The dye behaved similarly in all experiments.

Immunohistochemical labeling of live cells. This protocol was based on previously published protocols (17–19). The cells were neither fixed nor permeabilized. Cultured cells were washed once with warm (37°C) wash solution: external buffer (see above) supplemented with 0.5% BSA. Cells were then stimulated using the same high-potassium solution described above containing 0.5% BSA and polyclonal anti-insulin antibodies (1:50 dilution, guinea pig; Zymed, South San Francisco, CA). After 2 min, the stimulating solution was replaced with ice-cold wash buffer, and cell chambers were placed on ice, where they remained until cells were viewed. Cells were washed three times and then stained with a fluorescent secondary antibody (1:1,000 dilution, Alexa Fluor 488 goat anti-guinea pig; Invitrogen). After 20 min of staining, cells were once again washed three times. Cells were then imaged using the TIRF microscope described above. Regions of interest were first identified by imaging green fluorescence from the secondary antibody. These regions were then counterstained with fluorescent zinc dye using a micropipette to transiently apply extracellular solution spiked with a low concentration of zinc dye (5 μmol/l Rhodzin). When Alexa Fluor 488 goat anti–guinea pig antibody is viewed with the filters described above, red intensity is ~10% green intensity. For analysis of Rhodzin signals, we first subtracted the red fluorescence contributed by the green antibody. To assess objectively the overlap of anti-insulin antibody and Rhodzin, we constructed scattergrams by plotting the intensity of green and red fluorescence in each pixel. For each scattergram, a correlation coefficient was calculated.

Data analysis. To quantify the size of individual fluorescent spots, we fit their fluorescence profiles to a Gaussian curve: $y = y^0 + A^* \exp(-(x - \mu)^2/2\sigma^2)$, using an algorithm written in MatLAB (Mathworks, Natick, MA); the diameter was taken as two times the parameter, σ, returned as the best-fit coefficient for the Gaussian curve. All data are reported as means ± SE. In all figures, fluorescence intensity traces for single vesicles were corrected for local background. Error bars show SE for each point. A two-tailed Student's *t* test was used to test for significant differences.

RESULTS

Native cargo leaves insulin vesicles at widely varying rates. To study exocytosis of single insulin vesicles, we prepared primary cultures of human and rat pancreatic β-cells. We selected small clusters of cells for study and bathed them in a membrane-impermeant fluorescent zinc indicator. Fluorescent zinc indicators have previously been shown to report single insulin–vesicle exocytosis (28). We used TIRF microscopy, a method by which fluorescence is confined to a thin slice in the aqueous region just above the glass coverlip (29), making it ideal for imaging processes near the plasma membrane.

When cells bathed in fluorescent zinc indicator were exposed to a high-potassium ion concentration (50 mmol/l), fluorescence intensity increased suddenly (Fig. 1*B* and *C*). Such rapid and intense changes can occur only after vesicles fuse, because the fluorescent zinc indicator is membrane impermeant and is applied outside of the cell.

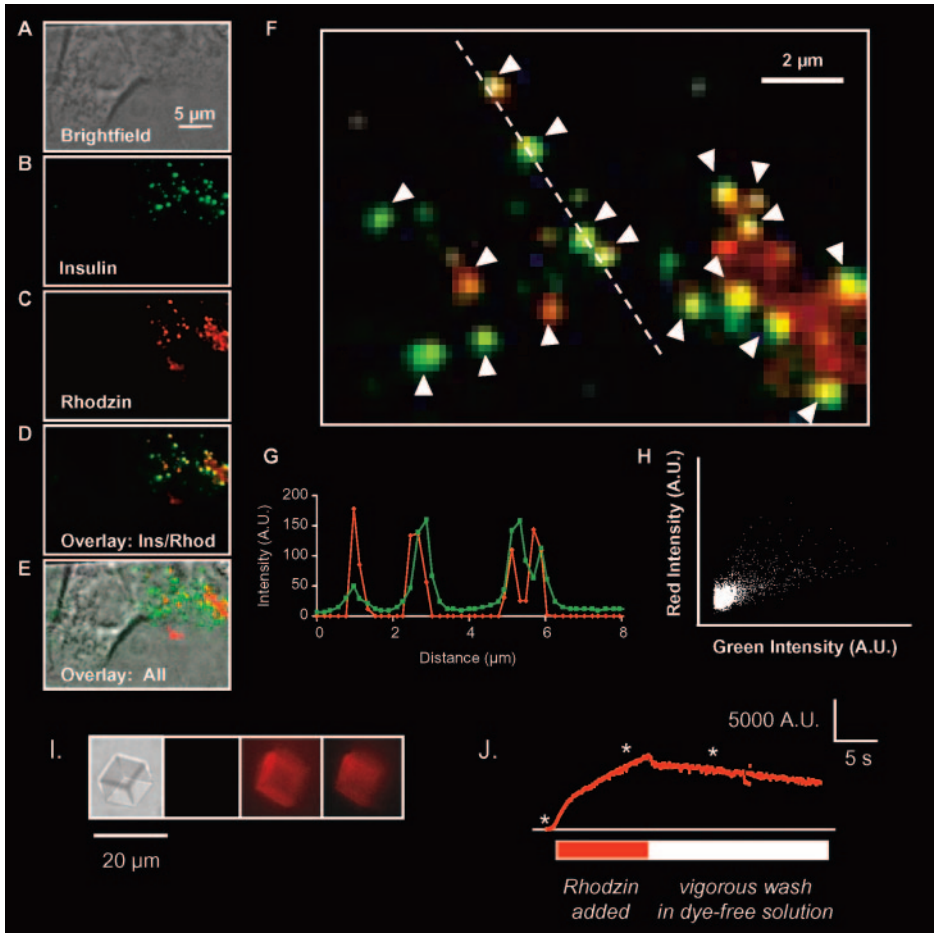

FIG. 3. Fluorescent zinc dye stains extracellular insulin-dense cores and insulin crystals. *A*: Brightfield (*A–E*, same intensity scale). *B*: Insulin. *C*: Rhodzin. *D*: Overlay of *B* and *C*. *E*: Overlay of *A–C*. *F*: A region from *D*. *G*: Fluorescence intensity traces taken over the dashed white line in *F*. *H*: Scattergram of red and green fluorescence intensities in *F*. *I*: Four images of a single insulin-zinc crystal: *first panel*: bright field image before the red fluorescent zinc indicator Rhodzin was applied, *second panel*: fluorescence image before Rhodzin was applied, *third panel*: fluorescence image while Rhodzin was applied, and *fourth panel*: fluorescence image during vigorous wash period. The three fluorescence images are shown on the same intensity scale and were taken at the times indicated by the asterisks shown in *J*. *J*: Fluorescence intensity in a region of interest at the center of the crystal.

Most fluorescence changes appeared punctate. We classified individual spots into three readily distinguished categories: *1*) transient diffuse clouds (Fig. 1*D*), *2*) short-lived vesicle-sized spots (Fig. 1*E*), and *3*) long-lived vesicle-sized spots (Fig. 1*F*).

Events in the first category, the transient diffuse clouds, had rapidly expanding diameters and short durations. Typically, the diameters of these expanding clouds changed from frame to frame, reaching >2 μm in at least one frame before disappearing. The lifetimes of these clouds ranged from 200 to 400 ms. Events in this category are consistent with the fluorescence changes observed by Qian et al. (28).

The events described in categories 2 and 3 were not previously reported. Events in categories 2 and 3 featured a small spot of fluorescence that sometimes appeared at first surrounded by a rapidly dispersing cloud (Fig. 1*F*, arrow highlights a cloud). The mean diameter of these small spots was indistinguishable from the mean diameter of insulin vesicles labeled with fluorescent cargo proteins and visualized with the same imaging system (280 ± 50 nm, n = 48 spots, five cells vs. 300 ± 50 nm, n = 50, five cells, respectively, see below [Fig. 4*B* and *C*]). Events in category 2 were distinguished from those in category 3 by the lifetime of the spot. Events in category 2 featured short-lived vesicle-sized spots that typically appeared and disappeared in a period lasting between 2 and 10 s (3.4 ± 0.4 s, 87 spots, eight cells, Fig. 1*G*). The fluorescent spots disappeared despite the maintained presence of the zinc dye, so the eventual disappearance of the spots does not represent gradual loss of dye ("destaining") from a persisting structure. Events in category 3 featured long-lived vesicle-sized spots that remained visible for >30 s (54 vesicles, eight cells).

Individual cells displayed widely varying secretion responses, with the numbers of newly appearing spots ranging from none to dozens. In the most vigorously responding cells, ~50 (45 ± 11, five cells) new spots appeared within 30 s after stimulating solution was applied. The magnitude of this response is similar to the magnitude of the response we previously observed (9) when we used fluorescent cargo proteins to detect exocytosis of single insulin vesicles (57 ± 17, five cells).

The fraction of fluorescent spots belonging to each category also varied widely from cell to cell. In general, ~60% of the events were either diffuse clouds or short-lived vesicle-sized spots, while the remaining 40% were long-lived vesicle-sized spots (87 and 54 of 141 vesicles, respectively, n = 8 cells). In these cells, there was no apparent correlation between the vigor of the cell's re-

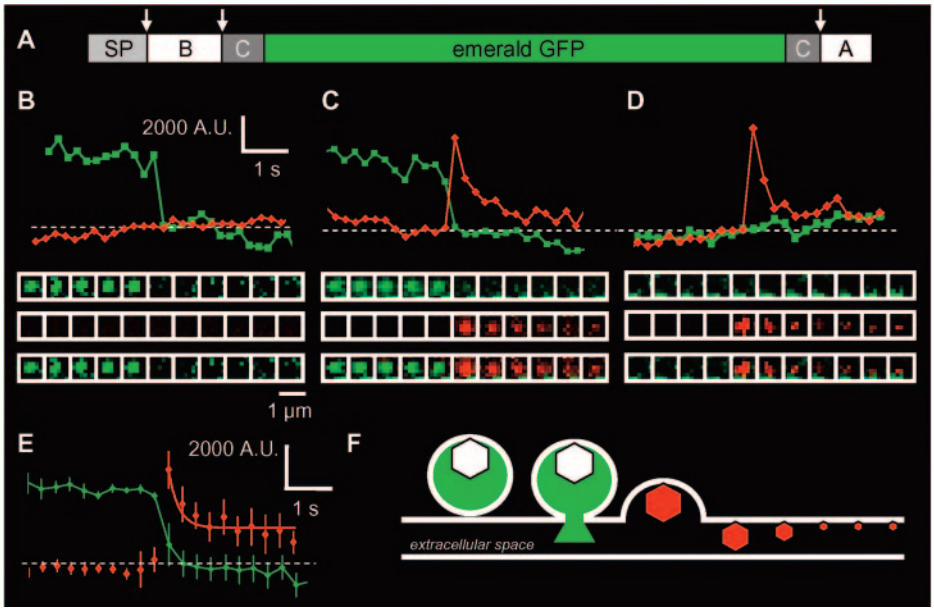

FIG. 4. C-peptide and insulin leave vesicles at different rates. *A*: Scale drawing of the four domains of preproinsulin with emerald GFP inserted in the middle of C-peptide. Arrows indicate processing sites. A, A-chain of mature insulin; B, B-chain of mature insulin; C, C-peptide processing fragment; SP, signal peptide (see also 22). *B–D*: Representative results for single vesicles (C-peptide [green] and zinc indicator [red]). *E*: Average secretion kinetics at overlapping sites of exocytosis (n = 8 vesicles). Smooth red trace shows a single exponential curve fitted to red data points, using $y = y^0 + A^0 \times exp\ (-t/\tau)$, where y = 1,200 arbitrary units, A^0 = 2,800 arbitrary units, and τ = 0.43 s. *F*: A model for one mode of insulin vesicle exocytosis: a mature insulin vesicle contains an insulin-zinc core surrounded by an acidic halo, which contains labeled C-peptide (green). After membrane fusion, labeled C-peptide is released and zinc indicator (red) can stain a slowly dissolving insulin-zinc core. This labeled core then dissolves with different rates and to different extents and may eventually be recaptured (not shown). The montages in *B–D* show consecutive images acquired at 0.28 s per frame.

sponse and the distribution of vesicles in the three categories.

These heterogeneous patterns of fluorescence change demonstrate that native cargo leaves insulin vesicles at widely varying rates. Similar results were obtained when we monitored secretion at planes above the coverslip (Fig. 2, *all panels*, and online appendix Fig. S1; rates of secretion: 1.5 ± 0.7 spots · μm^{-2} · min^{-1} [base of cell], n = 4 and 3 ± 1.6 spots · μm^{-2} · min^{-1} [between cells], n = 4).

Fluorescent zinc dye stains extracellular insulin-dense cores and insulin-zinc crystals. The short- and long-lived vesicle-sized spots described above suggest that insulin vesicle cargo sometimes disperses slowly during exocytosis. We used anti-insulin antibody to demonstrate that small spots on the plasma membrane of pancreatic β-cells that contain insulin are also stained by fluorescent zinc dyes (Fig. 3*A–F*).

Overlap of anti-insulin antibody and Rhodzin was assessed in two ways. First, the intensities of green and red fluorescence intensities in overlay images were compared along lines drawn through a number of fluorescent spots. The excellent correlation seen in Fig. 3*G* demonstrates that both anti-insulin antibody and Rhodzin recognize the same structures. Diameters of individual spots measured ~300 nm, similar to the size expected for insulin dense cores. Second, scattergrams constructed from corresponding pairs of red and green images revealed a strong correlation between red and green fluorescence intensities (Fig. 3*H*). These scattergrams assess the extent of fluorescence overlap throughout the images, not just along selected lines drawn through spots. The specificity of the correlation was demonstrated by rotating one of the images 180°. For the data shown, rotation of the red image lowered the correlation coefficient from 0.62 to 0.08. Data shown are representative of three similar fields (0.51 ± 0.09 vs. 0.09 ± 0.06, $P < 0.05$).

Fluorescent zinc dye also brightened significantly when applied in vitro to small crystals of insulin and zinc (Fig. 3*I* and *J*). The fluorescence intensity of the dye dimmed slowly during a vigorous wash period, suggesting that the dye enters the crystal and leaves it slowly.

These observations demonstrate that fluorescent zinc indicators stain insulin-zinc crystals including material from the dense core of insulin vesicles. Interestingly, the zinc dye does not stain the vesicle dense cores of adrenal chromaffin cells that have been stimulated to secrete, indicating some specificity in the staining of the insulin dense cores (not shown).

C-peptide and insulin leave vesicles at different rates. We next used two-color TIRF microscopy (24,25) to compare secretion kinetics for different types of cargo stored in the same insulin vesicle. To monitor release of dense-core cargo, we used the red fluorescent zinc indicator, Rhodzin, as described above. To monitor release of soluble proteins, we used a fluorescent cargo protein designed to deliver its fluorescent tag to the vesicle halo. For this probe, emerald GFP was inserted in the middle of the C-peptide fragment of preproinsulin, the insulin precursor polypeptide (Fig. 4*A*; see 22). As vesicles mature, the C-peptide fragment is removed from the precursor polypeptide and accumulates in the vesicle halo (4). The fluorescence intensity of emerald GFP shows little sensitivity to the large pH change that occurs during exocytosis (10). Thus, this marker is equally detectable before, during, and after exocytosis. Previously, we have shown that during exocytosis this particular fluorescently tagged protein consistently leaves insulin vesicles rapidly (<200 ms) and completely (9). Because GFP is much larger than insulin monomer, release of the fluorescently tagged C-peptide indicates when the fusion pore formed during exocytosis has dilated sufficiently so that freely diffusing

insulin and other cargo proteins should also be able to escape (10).

Human and rat primary cultured pancreatic β-cells expressing labeled C-peptide were bathed in Rhodzin. Upon stimulating these cells, we observed single vesicle exocytosis at many sites, scattered about in all regions of the cell's footprint. Individual sites were identified either by rapid secretion of labeled C-peptide (Fig. 4*B* and *C*) or by staining of the condensed core with Rhodzin (Fig. 4*C* and *D*) or by both (Fig. 4*C*). As in our previous study, labeled C-peptide always left vesicles rapidly and completely. Generally, the number of vesicles fusing varied widely from cell to cell, as was seen in previous experiments using Rhodzin alone or fluorescently tagged C-peptide alone. There was only moderate overlap between the sites of vesicle fusion marked by release of labeled C-peptide and those sites marked by Rhodzin's staining of a condensed core. A moderate correlation between the markers of exocytosis was expected, because only a fraction of insulin vesicles contained the fluorescent cargo protein. The fraction of insulin vesicles that contain fluorescent cargo protein varies from cell to cell and is determined by the lifetime of an insulin vesicle and the time allowed between infecting cells and imaging secretion (see DISCUSSION).

In human pancreatic β-cells expressing labeled C-peptide, Rhodzin-labeled cores appeared at one-third of sites where labeled C-peptide vanished (33 of 99, $n = 8$ cells; compare Fig. 4*B* and *C*). This percentage varied widely among individual cells, ranging from a high of 85% (16 of 17 vesicles) to a low of 0% (0 of 7 vesicles). When both fluorescent markers reported exocytosis at the same site, there were two noteable features. First, the lifetimes of stained cores varied widely (red trace in Fig. 4*C* and *E*) just as they did for vesicles lacking labeled C-peptide (Figs. 1*D–F*). Second, we never observed staining of an insulin-dense core before we observed disappearance of fluorescently tagged C-peptide. Rather, in every case, we observed complete release of labeled C-peptide and staining of the insulin-dense core within one frame (<300 ms) of one another.

When viewed with the rest of our data, these results show that C-peptide and insulin leave vesicles at different rates (Fig. 4*F*). Rhodzin-stained cores also dissolved with widely varying rates at sites of exocytosis identified by expression of cytoplasmic fluorescent protein (online appendix Fig. S2).

DISCUSSION

In the present study, we have investigated the fate of cargo released from individual insulin vesicles in primary cultures of rodent and human pancreatic β-cells. Using a combination of fluorescent probes located both inside and outside of vesicles, we compared secretion kinetics for different components of cargo stored in the same vesicle. We have demonstrated that the rate and extent of release for native insulin vesicle cargo vary widely, even among vesicles stored in the same cell. Specifically, we showed that C-peptide consistently leaves insulin vesicles rapidly and completely, while other components of native vesicle cargo including insulin leave vesicles at widely varying rates and to widely varying extents. We conclude that the population of insulin vesicles is heterogeneous with respect to how rapidly their cargo disperses.

Imaging slow dispersion of an insulin-dense core. The cargo in insulin vesicles has long been thought to partition between two distinct physicochemical phases: a solution with many ions, small molecules, and proteins and a dense core composed primarily of insulin and zinc (30). Moreover, in most species, including humans, the insulin-dense core is believed to be crystalline (31). However, methods have not been previously available to study in real time the fate of the secreted dense core. The main challenge for such a measurement has been devising a way to label the dense core without perturbing it.

Here, we have measured the release rates for native insulin vesicle cargo, including the dense core, by taking advantage of fluorescent zinc indicators that brighten when they encounter a crystal of insulin and zinc. The ability of fluorescent zinc indicators to stain crystals of insulin and zinc makes them very useful probes for measuring dispersion of an insulin vesicle's native cargo. Because we applied the fluorescent zinc indicators continuously in our experiments to measure insulin vesicle exocytosis, the fluorescence changes for the zinc indicator reflect the amount of insulin-zinc crystal remaining at a site of exocytosis and fluorescence decreases do not reflect loss of dye from the dense core.

Our results confirm that insulin vesicles store their cargo in at least two functionally distinct compartments. As previously reported (9–12,25,28), the contents of one compartment (labeled with fluorescently tagged C-peptide) behaved like a fluid phase that escaped rapidly and completely after vesicles fused with the plasma membrane (green traces in Fig. 4*B*, *C*, and *E*). If there were no dense core and the cargo in the fluid phase was freely diffusing, simulations of exocytosis indicate that release material would fully disperse in only milliseconds (32). However, the appearance of a fluorescent spot (labeled with bath-applied Rhodzin) that dissipated over times spanning at least two orders of magnitude (red traces in Fig. 4*C-E*) suggests that the contents of the second compartment behaved as a slowly dissolving condensed phase. As highlighted by the short-lived vesicle-sized spots (Fig. 4*C*), the slow release of Rhodzin-labeled insulin-containing cores could not be attributed solely to slow expansion of the initial fusion pore (but compare ref. 10 with 33), because molecules larger than insulin monomer (fluorescently tagged C-peptide) escaped long before some cores fully dispersed (Fig. 4*C* and *E*). The long-lived vesicle-sized spots (Fig. 1*F*), however, are consistent with resealing of insulin vesicles, whose dense cores were stained by Rhodzin during transient fusion, a mode of secretion recently observed for insulin vesicles (13,34–36).

The amount of slowly dissolving condensed cargo stored in each vesicle varied widely. In our experiments, it was possible to quantify the fraction of newly synthesized vesicles (≤48 h old, the maximum time between infecting cells and imaging secretion) that released slowly dissolving insulin. For this calculation, we assumed that every insulin vesicle was labeled with fluorescent cargo protein after the cell began expressing fluorescent cargo protein. In this population of young vesicles, about one-third of the vesicles undergoing exocytosis contained slowly dissolving condensed cargo (Fig. 4*C*), and two-thirds did not (Fig. 4*D*). When insulin vesicles release fluorescently tagged C-peptide, Rhodzin has access to the vesicle's interior, because the dye is much smaller than GFP and the dye is surrounding the cell throughout the experiment. Thus, it seems likely that the two-thirds of sites where a vesicle

released fluorescently tagged C-peptide without being labeled by Rhodzin (Fig. 4*D*) represent sites where vesicles are releasing insulin that is stored in a rapidly dispersing form. Alternatively, it is possible that Rhodzin does not brighten at these sites, because it is excluded from the insulin-dense core through a mechanism other than the restrictive size of the fusion pore. This alternative mechanism would be consistent with selective release of cargo stored in the vesicle halo, as reported most recently by Obermuller et al. (34). Tsuboi and Rutter (13) have also reported that many insulin vesicles fuse transiently with the plasma membrane and retain large amounts of fluorescently tagged cargo proteins (see comments below).

At some sites where Rhodzin stained an insulin dense core, there was no release of fluorescent C-peptide (Fig. 4*D*). It is important to make clear that there was no fluorescent C-peptide visible at any of these locations before the Rhodzin-stained spot appeared. At least two mechanisms could explain this observation. First, it may be that a vesicle that was made before we infected the cells with adenovirus has fused with the plasma membrane. We imaged secretion within 48 h after infecting cells, yet the lifetime of insulin vesicles is many days. Thus, any vesicles older than 48 h are not expected to contain fluorescent cargo protein and will not release fluorescent cargo protein when they fuse with the plasma membrane. Alternatively, the appearance of a Rhodzin-stained spot without the simultaneous release of fluorescent cargo protein could be evidence for multiple rounds of exocytosis for a single insulin vesicle. According to this model, in the first round of exocytosis, all of the fluorescent cargo protein would be released, but the insulin-dense core would not be stained by Rhodzin. Staining of the dense core with Rhodzin would instead occur in the second round of exocytosis.

From these experiments, it is clear that the composition of cargo varies widely among the population of membrane-proximal insulin vesicles. Furthermore, even among the vesicles containing condensed cargo, the cargo was released at widely varying rates during exocytosis, sometimes dissipating rapidly and at other times taking many seconds or even minutes to dissipate (Fig. 4*F*). This finding leads us to our most important conclusion: pancreatic β-cells secrete insulin in fast- and slow-release forms.

Do insulin vesicles kiss and run? Some recent imaging studies (13,34,35) have suggested that the majority of insulin vesicles use a kiss-and-run mechanism of secretion; that is, the vesicles fuse transiently with the plasma membrane before being retrieved intact into the cell. According to this model, the amount of material released by a vesicle during transient fusion is determined by the size and duration of the fusion pore. When discussing mechanisms of exocytosis, it is useful to distinguish the behavior of the vesicle membrane from the behavior of the vesicle cargo. Discussions focusing on the behavior of the vesicle cargo might also benefit by distinguishing different types of cargo, i.e., dense core versus halo or native versus foreign. Here, we have compared the behavior of cargo stored in the vesicle halo and cargo stored in the condensed core; moreover, we have also compared the behaviors of foreign and native cargo. We have not, however, examined how membrane added to the plasma membrane during exocytosis is later retrieved. Thus, we cannot comment on the importance of kiss-and-run secretion for insulin vesicle exocytosis. As stated above, the long-lived vesicle-sized spots we observed are consistent with kiss-and-run exocytosis. From our experiments, however, we can conclude only that most insulin vesicles release all of their cargo rapidly and completely during exocytosis. Results from other studies demonstrated that some vesicle membrane proteins do not disperse during exocytosis and are later retrieved intact (37).

Conclusions and biological significance. In the present work, we monitored the fate of the insulin-dense core after exocytosis, using an approach that did not require the introduction of a foreign fluorescent protein marker into the regulated secretory pathway. This technical advance is especially important for pancreatic β-cells, because the behavior of fluorescently tagged proteins in these cells is poorly understood (9) and may not report the behavior of native insulin.

We have directly shown for the first time that single insulin vesicles release their cargo with complex secretion kinetics, suggesting that among vesicles undergoing exocytosis the cargo exists in heterogeneous physical states. Our work suggests that not only are the contents partitioned in some vesicles into at least two states, a soluble phase and a less-soluble phase, but the less-soluble phase exists in different states. The less-soluble phase most likely represents a crystalline dense core, where most insulin is stored. In addition, there are many vesicles whose contents are released rapidly and completely and do not appear to have a slowly dissolving dense core.

By populating the readily releasable pool of insulin vesicles with a mixture of vesicles whose cargo disperse at various rates, a pancreatic β-cell has the capacity to release insulin with a complex time course that extends well beyond the time of vesicle fusion. When sampled in the portal vein, physiological insulin release appears as a series of narrow pulses (<2 min per pulse) occurring every 5 to 10 min and superimposed on a lower basal rate of release (38). The secretion pulses have been attributed to transient bursts of action potentials in β-cells that lead to calcium entry via voltage-gated calcium channels and to insulin exocytosis (39,40). Between bursts, very little or no insulin secretion is believed to take place. We speculate that between the bursts of vesicle fusion that underlie the pulses of secretion, the dense cores that were released during a preceding burst continue to release insulin as they dissolve. The low basal release rate provided by the slowly dissolving insulin dense core would ensure the presence of insulin at all times, thus preventing the metabolic complications of insulin deficiency.

ACKNOWLEDGMENTS

Funding for this work was provided by grants from the U.S. National Institutes of Health to D.J.M. (DK10181) and R.H.C. (DK60623). Human islets for basic research were made available by the Islet Cell Resource Centers (City of Hope, Duarte, CA).

We thank Peter Butler, Lou Byerly, Ray Boston, Maryann Vogelsang, and Dorte Madsen for helpful discussions. We thank Kalpit Gajeera for providing analysis software. We thank all members of the Islet Cell Resource Center for their time and efforts.

REFERENCES

1. Bergman RN, Ader M, Huecking K, Van Citters G: Accurate assessment of β-cell function: the hyperbolic correction. *Diabetes* 51 (Suppl. 1):S212–S220, 2002
2. Weir GC, Bonner-Weir S: Five stages of evolving β-cell dysfunction during progression to diabetes. *Diabetes* 53 (Suppl. 3):S16–S21, 2004

3. Hutton JC, Penn EJ, Peshavaria M: Low-molecular-weight constituents of isolated insulin-secretory granules: bivalent-cations, adenine-nucleotides and inorganic-phosphate. *Biochem J* 210:297–305, 1983
4. Michael J, Carroll R, Swift HH, Steiner DF: Studies on the molecular-organization of rat insulin secretory granules. *J Biol Chem* 262:16531–16535, 1987
5. Njus D, Kelley PM, Harnadek GJ: Bioenergetics of secretory vesicles. *Biochim Biophys Acta* 853:237–265, 1986
6. Dodson G, Steiner D: The role of assembly in insulin's biosynthesis. *Curr Opin Struct Biol* 8:189–194, 1998
7. Hutton JC: Secretory granules. *Experientia* 40:1091–1098, 1984
8. Arvan P, Halban PA: Sorting ourselves out: seeking consensus on trafficking in the beta-cell. *Traffic* 5:53–61, 2004
9. Michael DJ, Geng X, Cawley NX, Loh YP, Rhodes CJ, Drain P, Chow RH: Fluorescent cargo proteins in pancreatic beta cells: design determines secretion kinetics at exocytosis. *Biophys J* 87:L3–L5, 2004
10. Barg S, Olofsson CS, Schriever-Abeln J, Wendt A, Gebre-Medhin S, Renstrom E, Rorsman P: Delay between fusion pore opening and peptide release from large dense-core vesicles in neuroendocrine cells. *Neuron* 33:287–299, 2002
11. Ma L, Bindokas VP, Kuznetsov A, Rhodes C, Hays L, Edwardson JM, Ueda K, Steiner DF, Philipson LH: Direct imaging shows that insulin granule exocytosis occurs by complete vesicle fusion. *Proc Natl Acad Sci U S A* 101:9266–9271, 2004
12. Ohara-Imaizumi M, Nakamichi Y, Tanaka T, Ishida H, Nagamatsu S: Imaging exocytosis of single insulin secretory granules with evanescent wave microscopy: distinct behavior of granule motion in biphasic insulin release. *J Biol Chem* 277:3805–3808, 2002
13. Tsuboi T, Rutter GA: Multiple forms of "kiss-and run" exocytosis revealed by evanescent wave microscopy. *Curr Biol* 13:563–567, 2003
14. Figlewicz DP, Forhan SE, Hodgson AT, Grodsky GM: Zn-65 and endogenous zinc content and distribution in islets in relationship to insulin content. *Endocrinology* 115:877–881, 1984
15. Gold G, Grodsky GM: Kinetic aspects of compartmental storage and secretion of insulin and zinc. *Experientia* 40:1105–1114, 1984
16. Rubenstein AH, Clark JL, Melani F, Steiner DF: Secretion of proinsulin C-peptide by pancreatic beta cells and its circulation in blood. *Nature* 224:697–699, 1969
17. Kaplan DR, Colca JR, McDaniel ML: Insulin as a surface marker on isolated cells from rat pancreatic-islets. *J Cell Biol* 97:433–437, 1983
18. Larsson LI, Nielsen JH, Hutton JC, Madsen OD: Pancreatic hormones are expressed on the surfaces of human and rat islet cells through exocytotic sites. *Eur J Cell Biol* 48:45–51, 1989
19. Leung YM, Sheu L, Kwan E, Wang G, Tsushima R, Gaisano H: Visualization of sequential exocytosis in rat pancreatic islet beta cells. *Biochem Biophys Res Commun* 292:980–986, 2002
20. Sondergaard LG, Stoltenberg M, Flyvbjerg A, Brock B, Schmitz O, Danscher G, Rungby J: Zinc ions in beta-cells of obese, insulin-resistant, and type 2 diabetic rats traced by autometallography. *APMIS* 111:1147–1154, 2003
21. Qian WJ, Aspinwall CA, Battiste MA, Kennedy RT: Detection of secretion from single pancreatic beta-cells using extracellular fluorogenic reactions and confocal fluorescence microscopy. *Anal Chem* 72:711–717, 2000
22. Watkins S, Geng X, Li L, Papworth G, Robbins PD, Drain P: Imaging secretory vesicles by fluorescent protein insertion in propeptide rather than mature secreted peptide. *Traffic* 3:461–471, 2002
23. Wrede CE, Dickson LM, Lingohr MK, Briaud I, Rhodes CJ: Protein kinase B/Akt prevents fatty acid-induced apoptosis in pancreatic beta-cells (INS-1). *J Biol Chem* 277:49676–49684, 2002
24. Taraska JW, Perrais D, Ohara-Imaizumi M, Nagamatsu S, Almers W: Secretory granules are recaptured largely intact after stimulated exocytosis in cultured endocrine cells. *Proc Natl Acad Sci U S A* 100:2070–2075, 2003
25. Tsuboi T, Zhao C, Terakawa S, Rutter GA: Simultaneous evanescent wave imaging of insulin vesicle membrane and cargo during a single exocytotic event. *Curr Biol* 10:1307–1310, 2000
26. Kaarsholm NC, Ko HC, Dunn MF: Comparison of solution structural flexibility and zinc-binding domains for insulin, proinsulin, and miniproinsulin. *Biochemistry (Mosc)* 28:4427–4435, 1989
27. Steiner DF: Cocrystallization of proinsulin and insulin. *Nature* 243:528–530, 1973
28. Qian WJ, Gee KR, Kennedy RT: Imaging of Zn2+ release from pancreatic beta-cells at the level of single exocytotic events. *Anal Chem* 75:3468–3475, 2003
29. Axelrod D: Selective imaging of surface fluorescence with very high aperture microscope objectives. *J Biomed Opt* 6:6–13, 2001
30. Orci L: Banting Lecture 1981: Macro-domains and microdomains in the endocrine pancreas. *Diabetes* 31:538–565, 1982
31. Greider MH, Howell SL, Lacy PE: Isolation and properties of secretory granules from rat islets of Langerhans. II. Ultrastructure of the beta granule. *J Cell Biol* 41:162–166, 1969
32. Chow RH, Von Ruden L: Electrochemical detection of secretion from single cells. In *Single-Channel Recording*. 2nd ed. Sakmann B, Neher E, Eds. New York, Plenum (Springer), 1995, p. 245–275
33. Takahashi N, Kishimoto T, Nemoto T, Kadowaki T, Kasai H: Fusion pore dynamics and insulin granule exocytosis in the pancreatic islet. *Science* 297:1349–1352, 2002
34. Obermuller S, Lindqvist A, Karanauskaite J, Galvanovskis J, Rorsman P, Barg S: Selective nucleotide-release from dense-core granules in insulin-secreting cells. *J Cell Sci* 118:4271–4282, 2005
35. Tsuboi T, McMahon HT, Rutter GA: Mechanisms of dense core vesicle recapture following "kiss and run" ("cavicapture") exocytosis in insulin-secreting cells. *J Biol Chem* 279:47115–47124, 2004
36. Kwan EP, Gaisano HY: Glucagon-like peptide 1 regulates sequential and compound exocytosis in pancreatic islet β-cells. *Diabetes* 54:2734–2743, 2005
37. Ohara-Imaizumi M, Nakamichi Y, Tanaka T, Katsuta H, Ishida H, Nagamatsu S: Monitoring of exocytosis and endocytosis of insulin secretory granules in the pancreatic beta-cell line MIN6 using pH-sensitive green fluorescent protein (pHluorin) and confocal laser microscopy. *Biochem J* 363:73–80, 2002
38. Song SH, McIntyre SS, Shah H, Veldhuis JD, Hayes PC, Butler PC: Direct measurement of pulsatile insulin secretion from the portal vein in human subjects. *J Clin Endocrinol Metab* 85:4491–4499, 2000
39. Bertram R, Satin L, Zhang M, Smolen P, Sherman A: Calcium and glycolysis mediate multiple bursting modes in pancreatic islets. *Biophys J* 87:3074–3087, 2004
40. Rorsman P, Renstrom E: Insulin granule dynamics in pancreatic beta cells. *Diabetologia* 46:1029–1045, 2003